Research Article   **Open Access**

U-Pb Zircon Age: Preliminary Data Evaluating the Earth History Recorded by Two Basement Rocks (Granitic Pegmatite and Mica-Schist) in Mamfe Basin (Sw Cameroon, Central Africa)

Nguo Sylvestre Kanouo[1]*, Emmanuel NjonFang[2], Arnaud Patrice Kouske[3], Rose Fouateu Yongue[4] and Gabriel Ngeutchoua[4]

[1]*Mineral Exploration and Ore Genesis Unit, Department of Mines and Quarries, Faculty of Mines and Petroleum Industries, University of Maroua, 46, Maroua-Cameroon*
[2]*Higher Teachers Training School, University of Yaoundé I, Cameroon*
[3]*Department of Civil Engineering, The University Institute of Technology, University of Douala, Cameroon*
[4]*Department of Earth Sciences, Faculty of Science, University of Yaoundé I, Cameroon*

Abstract

Zircon crystals from two basement rocks (granitic pegmatite and mica-schist) in the Mamfe Basin were studied to provide petrogenetic and geochronologic constraints, therefore were characterized and dated by LA-Q-ICP-MS analytical techniques, after their internal textural features were determined.

Zircon crystals with oscillatory zoning from the granitic pegmatite exceed 200 μm are mainly euhedral to prismatic. The U (≤169 ppm), Th (≤240 ppm), and Th/U (0.6-1.7) are within the range of zircon crystallized in crustal magmatic environment. The $^{206}Pb/^{238}U$ ages (506±11 to 639±25 Ma) and $^{207}Pb/^{235}U$ (490±13 to 653±29 Ma) date Early Precambrian (Early Neoproterozoic: Edicaran) to Cambrian event. They are close to the age of rocks crystallized during the Pan-African collision found within the Cameroon Mobile Belt.

Zircon crystals from the mica-schist are <100 to >200 μm in size, have magmatic (e.g., euhedral prismatic with oscillatory zone) and metamorphic (e.g., form round soccer ball, sub-hedral with overgrowth) features. The U (23-687 ppm), Th (4.0-161 ppm), and Th/U (0.01-1.8) are compatible with values in metamorphic and magmatic zircon crystallized within crustal environment. The highly heterogeneous $^{206}Pb/^{238}U$ (543 ± 12-2019 ± 30 Ma) and $^{207}Pb/^{235}U$ (526 ± 12-2008 ± 18Ma) mainly date Paleoproterozoic, Mesoproterozoic, and Neoproterozoic magmatic and/or metamorphic events.

Keywords: Mamfe Basin; Granitic pegmatite; Mica-schist; Zircon; Internal feature; Geochronology; Genesis

Introduction

Zircon (ZrSiO$_4$) is a common accessory mineral that occurs in a wide variety of sedimentary, igneous, and metamorphic rocks and very commonly occurs in consolidated to unconsolidated clastic deposits. It is chemically resistant and refractory, surviving weathering and transport processes, as well as high temperature metamorphism and anatexis [1]. Its relative insolubility in crustal melts and fluids, as well as its general resistance to chemical and physical breakdown, often result in the existence of several generation processes in a single zircon grain [2]. It presents external and internal features useful for its characterization [3-5]. It can incorporate fluid/melt (e.g., vapor bubbles, and glass) [6,7] and other minerals (e.g., biotite, quartz, feldspar, magnesian calcite, uraninite, apatite, galena, garnet, diamond, monazite, coesite, and omphacite) in their structure during crystal growth [5,8-10]. Zircon is the most widely used mineral for the extraction of information on the pre-history and genesis of magmatic, metamorphic, and sedimentary rocks [5,11]. Much of the geological usefulness of zircon stems from its suitability as a geochronometer, based on the decay of U and Th to Pb [12-15]. It is also the major host of radiogenic isotopic tracer Hf, and is used to determine oxygen isotopic compositions and REE, and other trace element abundances, all of which yield useful clues concerning the history of the host rock, and in some cases, the parent rock in which the zircon crystallized [4,16]. U-Pb dating of zircon has long been used to unravel the timing of tectonic events and related processes, including orogenic episodes and regional metamorphism. It is also used to determine the thermal history of rocks [14,17].

The Mamfe Basin in the SW region of Cameroon is an intracontinental sedimentary structure mainly filled with Cretaceous age immature and mature siliciclastic rocks [18-23]. These rocks overlay least studied assumed Precambrian magmatic and metamorphic rocks (Figure 1) composed of granites, syenites, migmatites, gneisses, and mica-schists [18,20,21,24,25]. Most of those rocks are still undated, although they are generally considered as part of the Cameroon Mobile Belt of Precambrian age. Dating part of these rocks would be of a great scientific interest as it may help to understand the pre-sedimentary magmatic and metamorphic history in this basin. In this paper zircon textural analysis, selected trace element geochemistry, and U-Pb dating are used to evaluate the earth history registered by two basement rocks (Otu granitic pegmatite and Babi mica-schist). This study is a preliminary research work for future projects to understand the earth history in the entire Mamfe Sedimentary Basin, considered to be the least studied basin in the west and central African region.
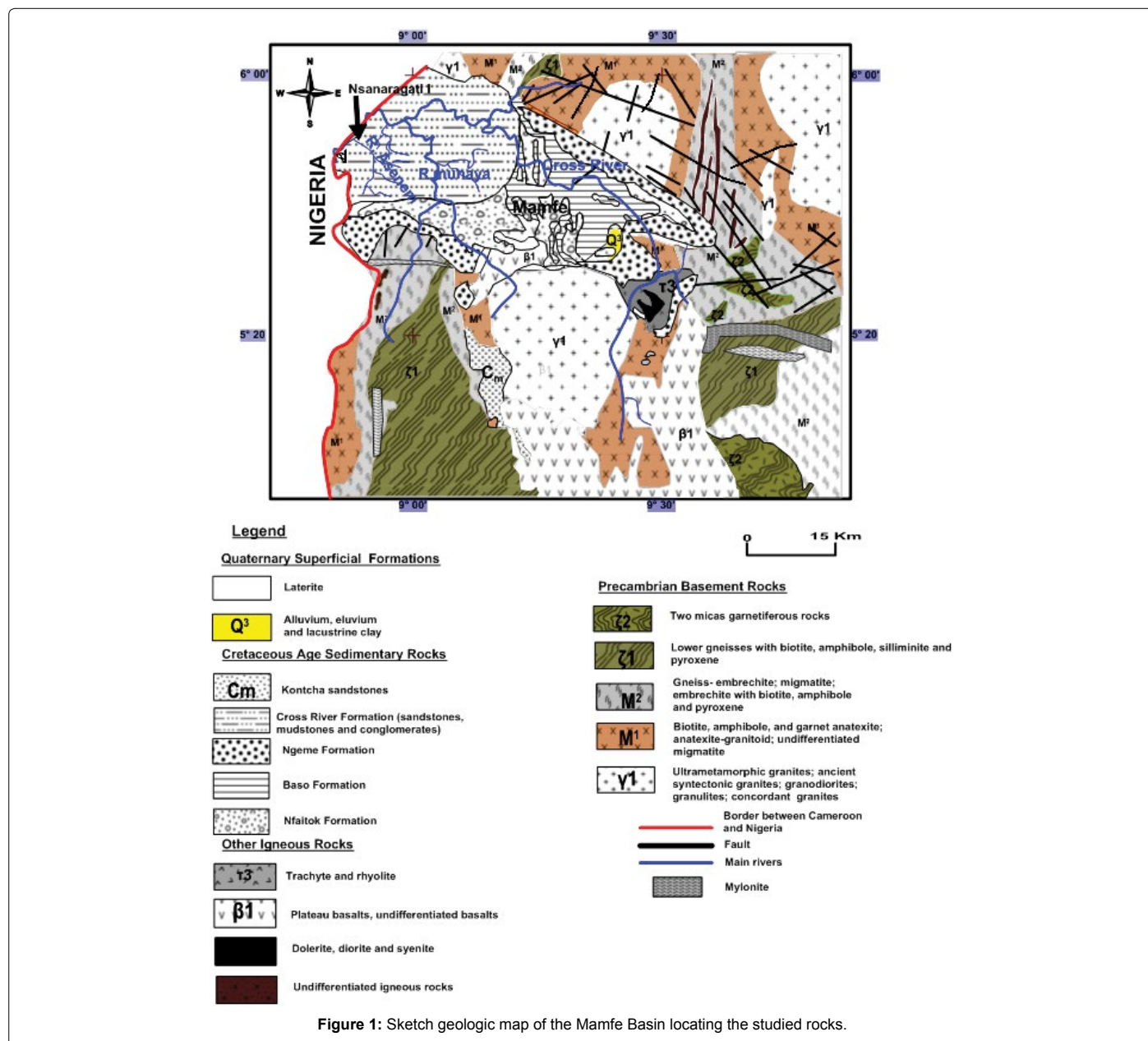
Figure 1: Sketch geologic map of the Mamfe Basin locating the studied rocks.

Review of Study in the Mamfe Basin and on Geochronology of the Cameroon Mobile Belt

Research studies carried out in the Mamfe Sedimentary Basin are summarized. A focus on the basement and the geochronological results obtained on rocks in the Cameroon Mobile Belt is summarized.

The mamfe basin

The Mamfe Sedimentary Basin is Cretaceous age depression whose subsidence is related to the rifting and formation the Atlantic Ocean [20,22,23]. This depression is filled with siliciclastic immature and mature sediments (shales, marlstones, siltstones mudstones, sandstones, and conglomerates) locally inter-bedded or associated with carbonates and volcaniclastic breccia rocks [18,20,22-28]. The ages for part of the lithified sediments in the Mamfe Basin range from

Aptian to Late Cenomanian (palinomorph ages: [22]) dating: (1, Late Cenomanian to probably Early Turonian) calcareous shale, limestone and silty and medium to coarse grained sandstone in the Nfaitok unit and lignitic black shale, calcareous shales and limestone at the Satome Bridge and (2, Aptian to Early Cenomanian or possibly Barremian) conglomeratic sandstones, conglomerates and shales at Okoyong. Other palynomorph ages (Barremian to Early Albian: [23]) date: Etoku Formation (made up of pre-rifting materials), Mamfe group (syn-rifting sediments) including Nfaitok Formation (fluvio-palustrine), Manyu Formation (lacustine), and Okoyong Formation (Fan-delta). Dinosaur trackways found on sandstones outcropping in Manyu River, precisely under the Nfaitok Bridge were dated Cenomanian to Turonian [28]. No ages were assigned for Ikom-Munaya Formation in the west due to lack of datable fossils [23]. The lithified clasts in the Mamfe Basin are locally associated with limestones and/or evaporites

[19,29,30]. The locale presence of evaporites (dominated by halite) suggests a late Aptian-early Albian marine ingression from the Douala Basin [23]. Part of very fine-grained siliciclastic rocks (shales) encloses organic matter with some petroleum potential [27]. Minerals such as galena are found associated with some of the immature sediment in the Mamfe Basin [31]. The lithified sediments are locally overlain by recent sediments sorted from volcanic, sedimentary, plutonic, and/or metamorphic rocks [24]. A fraction of these sediments notably those in the western part of the basin encloses economic viable heavy minerals (e.g., zircon, rutile, chrysoberyl, amethyst, corundum) from diverse origins [24,32-36]. Chrysoberyl, zircon, and part of the corundum were crystallized in magmatic plutonic rocks [32,34-36], whereas rutile grains were mainly grown in metapelitic metamorphic protoliths [33]. The crystallization age of zircons grains ranges from 11 to 1959 Ma with their sedimentation periods suggested being post-Serravallian, post-Eocene, post-Oligocene, and post-Miocene, post-Lower-Cretaceous, post-Neoproterozoic, and post-Paleoproterozoic [32,35]. The source of those clasts are suggested to be around the Cameroon Volcanic Line, Benue Trough, and part of the basement rock of the Mamfe Basin [24,32,35].

Sedimentary rocks in the Mamfe Basin are locally cross-cut or overlain by undated volcanic to sub-volcanic rocks (basalts, phonolites, trachytes, basanites, and picro-basalts) [18,20,21,24,37,38]. Alkaline, tholeiitic, and transitional basalts, basanites, and picro-basalts found in the west and southern part of the basin were mainly crystallized from less evolved mantle source magmas [38]. Those in the west (mainly basanite and picro-basalts) are alkaline to tholeiitic Ocean Island Basaltic rocks crystallized during post sedimentary tectono-volcanic activities [23,38]. The volcanic rocks in the Mamfe Basin and part of lithified sediments are underlain by Precambrian metamorphic (gneisses, mica-schists and migmatites), igneous (granites and syenites) [20,24]. Undated gabbro, granites, and syenites are associated with phonolite, trachytes, and hornfels in Mount Nda Ali found in the southeastern part this basin [37]. Part of the basement rocks are cross-cut by mafic and felsic dykes showing that those rocks were subject of post-emplacement fractured tectonism [37,24].

Geochronology of the cameroon mobile belt

The Cameroon Mobile Belt or Central African Fold Belt is a megatectonic structure underlying Cameroon, Chad, and Central African Republic between the Congo craton to the south and the Nigerian shield to the north [39]. It was formed during the Neoproterozoic from the collision between the Saharan metacraton and the Congo craton [40,41]. In Cameroonian territory, the Central African Fold Belt is made up of three main structural units: the Poli Group in its northern part, the Adamawa Group at the center, and the Yaoundé Group in the south [41]. Within the Central African Fold Belt several domains are recognized on the basis of field, petrographic, structural and isotopic studies. These include the Paleoproterozoic gneissic basement, Mesoproterozic to Neoproterozoic schists and gneisses of Poli, Yaoundé, and Lom, and Pan African granitoids whose ages range from the early stage of the deformation (orthogneisses) to the late uplift stages of the belts [42]. Examples of geochronological dating of those rocks include 520± 20 Ma for Poli and 498 ± 5 Ma for Lom (Rb-Sr age on whole–rock) [43], 525 Ma for Goutchoumi and 521 ± 19 Ma for Linté (Rb-Sr age on whole rock), 530 ±10 Ma and 510 ± 25 Ma, 569 ± 12 to 558 ± 24 Ma, and 533 ± 12 to 524 ± 28 Ma for Nkambe [44,45], 600 Ma for Ngondo [46], 620 ± 10 Ma for granulite in Yaoundé [47], 2.1 Ga paleoproterozoic for the garnet amphibolites and tonalitic to trondhjemitic gneisses, and 618 Ma magmatic rock of Tonga [48],

and 1617 ± 16 Ma (Paleoproterozoic in age) for the metasediments and 600 Ma for the monzodiorite of Bafia Group [49].

Field Description and Petrography of the Basement Rocks

The basement rocks (granitic pegmatite and mica-schist) from which the studied zircon crystals were taken are from two different localities (Otu: N05°28'13" and E008°57'26", in west and Babi: N05°28'13" and E008°57'26", in the south west). Information describing and characterizing those rocks are updated data from [24]. The first rock outcrops in Otu, south-west of Eymojock sub-division. It forms large and variable shape fragments spotted in soils mostly in the west and southern part of this village. It is the bed-rock of many lithified clasts found in this locality. This rock underlies conglomeratic sandstones in some rivers in the western part of the village. Petrographic data show that this inequigranular rock is macroscopically (Figure 2a) composed of very large feldspathic and quartz crystals, and spot of aggregates of mafic minerals dominated by biotite. Under the polarizing microscope (Figure 2b), it is composed of quartz (55%), plagioclase (20%), and K-feldspar (microcline and orthoclase) (15%), biotite (5%), clinopyroxene (2%), sericite (2%), and opaque minerals (1%). Quartz is inequigranular with very large anhedral grains (below 2
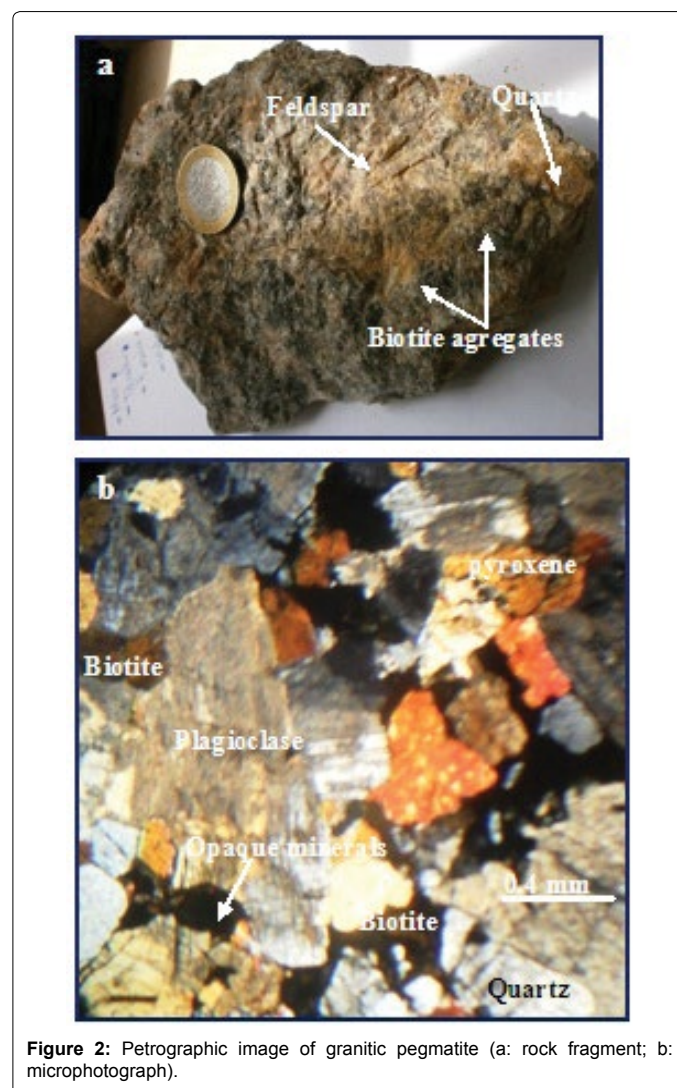

Figure 2: Petrographic image of granitic pegmatite (a: rock fragment; b: microphotograph).

mm to above 4 mm) and smaller size grains (below 2 mm). Some of the smaller quartz crystals are polycrystalline, typifying a re-crystallization. Plagioclase and K-feldspar form large laths (above 3 mm). Exsolution feature is visible in some alkali-feldspar. Biotite flakes (below 1 mm) locally enclose opaque minerals along the cleavage, showing oxidation due to weathering. These opaque minerals also occur within some crystals. Sericite forms micro-flakes found in some K-feldspar (sign of hydrothermal weathering of the K-feldspar). Clinopyroxene forms high-relief subhedral crystals.

Mica-schist is a slaty to weakly foliated rock found in Babi and Araru, which are two villages in the southwest of Eyumojock sub-division. This rock is generally covered by thick soils or virgin forestry vegetation. Few outcrops are found in some rivers (e.g., Akarem and tributries) and road-cuts. This rock is partly covered by a mafic flow in Araru. The mica-schist in Babi is composed of quartz, muscovite, and biotite. It is macroscopically similar to fragments from the Araru. Muscovite slates (up to 1 cm) are larger than those of biotite (below 4 mm). Under a polarizing microscope (Figure 3), Babi mica-schist is composed of quartz, muscovite, and biotite. It is locally banded with quartz-rich bands (up to 3.0 mm) alternating with mica-rich bands (up to 5.0 mm). Most quartz crystals are fractured. Polycrystalline quartz grains are common. Some crystals are elongated with pinch and swell feature. Porphyroblasts are visible with large quartz fractured crystals surrounded by mica flakes (Figure 3). Biotite and muscovite are folded, preferentially orientated or form wedges. Micas are intergranular or occur as fracture filling minerals (forming micro-veinlets). Some of those micro-veinlets cross-cut fabrics, showing a stockwork structure. The grano-porphyroblastic texture, the presence mylonites, polycrystalline quartz, kinked biotite, and folded muscovite in the Babi mica-schist show that this rock was probably affected by post-sedimentation tectono-metamorphic event(s).

Preparation and Zircon Analytical Techniques

The analyzed zircons were sampled from crushed granitic pegmatite and mica-schist collected, respectively in Otu and Babi regions. Sample preparation took place in Cameroon and China. Fragments were milled at the ALS mineral division laboratory in Mvan (Yaoundé). More than twenty kilograms of each sampled rocks were crushed. Maximum precaution was taken to avoid any contamination or mixture. Before milling, each sample was cleaned, chipped to reduce the size, and crushed. The milled samples were washed at the Department of Earth Sciences of the University of Yaoundé I, reducing the weight by eliminating part of the gangue (e.g., quartz and feldspar). Washed samples were placed in drying oven for 24 hours at 50°C, and later sent to China for mounting and CL imaging. The hand-pick crystals from each rock-type were mounted with epoxy resin on slide, and polished with abrasive to a standard thickness of 30 μm. The polished crystals were later exposed to cathodoluminescence imaging for determination of zircon internal texture at the State Key Laboratory in Geological Resources and Mineral Processes at the China University of Geosciences in Wuhan. The procedure used for acquisition of zircon internal feature is similar to that described in Corfu [5] where the images were taken using a CL detector attached to scanning electron microscopes (SEM-CL). The obtained zircon photos were later characterized follow criteria presented in Pupin [3] and Corfu [5].

The procedure used for U-Pb dating of those zircons is similar to that of McFarlane and Yan. The polished slabs were analyzed using modern 193 nm ArF excimer laser ablation (LA) and quadrupole inductively coupled plasma-mass spectrometry (Q-ICPMS). Data on Th, U, and Pb abundance and U-Pb age were obtained in craters (33 μm of diameter and < 20 μm of depth) dug in the core, rim, and oscillatory zones in each zircon crystal. They were obtained by combining enhanced ICP-MS sensitivity, fast and efficient sample cells, and sophisticated software controls, modern 193 nm ArF excimer LA-ICPMS systems.

Results

Internal morphological features, selected trace elemental (U, Th, and Pb) abundance, and U-Pb isotopic data and ages for each zircon crystal from Otu granitic pegmatite and Babi mica-schist are presented.

Internal features of zircon

The internal morphology of each zircon crystal and each rock type (Figures 4 and 5) is separately presented.

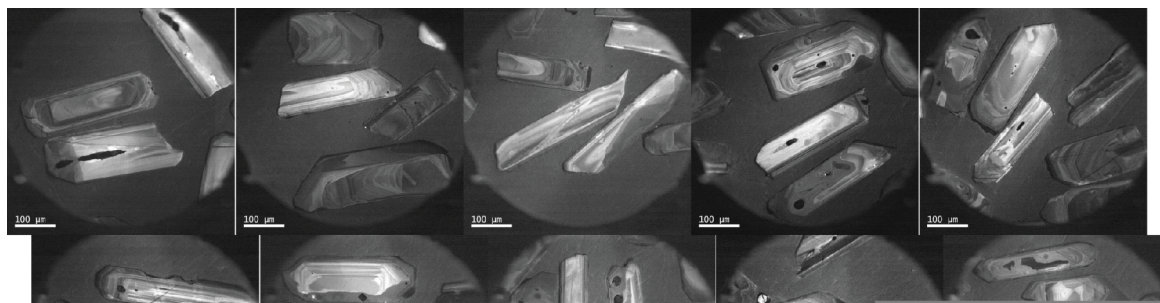

Figure 3: Microphotograph of mica-schist.

Figure 4: CL images showing the internal texture of zircon from Otu granitic pegmatitein south west of the Mamfe Basin, SW Cameroon.

Zircon from granitic pegmatite: The cathodoluminescence image of zircons from Otu granitic pegmatite in Figure 4 shows that they are euhedral having well-developed crystal faces. The crystal faces are mostly prismatic. Few crystal faces are pyramidal. Oscillatory zoning (common in magmatic zircons) [2] occurs in the crystals. The crystal size is generally above 250 μm within the range of magmatic zircon presented in Pupin [3].

Zircon from mica-schist: The internal image for zircon crystals from Babi mica-schist shows different morphology (Figure 5). They are euhedral with prismatic and/or pyramidal crystal faces, subhedral (just part of the crystal faces are developed), or form soccer ball or round and ovoid grains. Zircon fragments are also found. Overgrowth rim (metamorphic feature) [50] and conserved core are visible in some of the crystals. Growth zoning (feature common in magmatic zircon) [2] occurs in some crystals. The crystal size ranges from below 100 to more than 200 μm.

Trace element and U-Pb age

Selected trace element abundance and obtained U-Pb ages for each zircon crystal from Otu granitic pegmatite and Babi mica-schist are presented. They show some variation and heterogeneity mostly for crystals from the Babi mica-schist.

Zircon from Otu granitic pegmatite: The abundance of quantified trace elements (U, Th, and Pb: Table 1) in zircon from granitic pegmatite generally ranges from 16 to 169, 18 to 240, and 13 to 41 ppm, respectively. There is no important variation in U content in different spot realized in the same crystal, although for crystal Ot3 there is decrease in U. The observation is different for Th and Pb as these elements abundance dominantly decreases in nearly all zircon crystals. The calculated Th/U ratios range from 0.6 to 1.7 with most values being within the range limit in zircon growth in igneous felsic rocks published in Heaman [16].

The obtained U-Pb isotopic data presented in Table 1 show some variation. The $^{207}Pb/^{235}U$ ratios (> 0.6) are relatively higher than $^{206}Pb/^{238}U$ (0.08 to <0.12), $^{207}Pb/^{206}Pb$ (> 0.05), and $^{208}Pb/^{232}Th$ (≤ 0.01) ratios. The $^{206}Pb/^{238}U$ (506 ± 11 to 639 ± 25 Ma) and $^{207}Pb/^{235}U$ (490 ± 13 to 653 ± 29 Ma) ages for spots realized in each zircon crystal are variable. They date Early Precambrian (Early Neoproterozoic: Edicaran) to Cambrian event. The plotted data in Figure 6 show grouping of plots with three main distinguish age population: Edicaran to Cryogenian, Fortunian, and Jiangshanian to Fortunian groups. Some zircon (e.g., Ot1: ≈537 Ma and Ot5: ≈ 545 Ma) have the same $^{206}Pb/^{238}U$ age in two realized spots, whereas an age difference is noted in others.

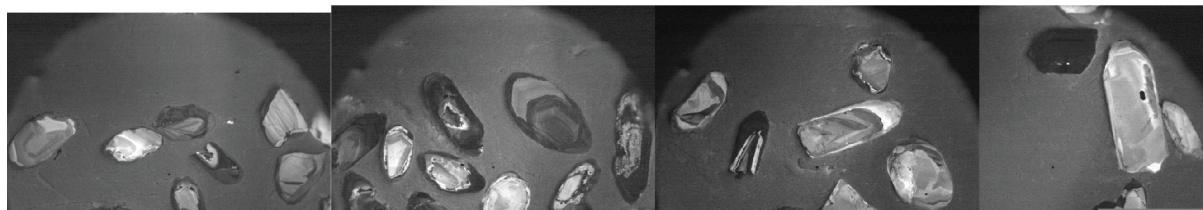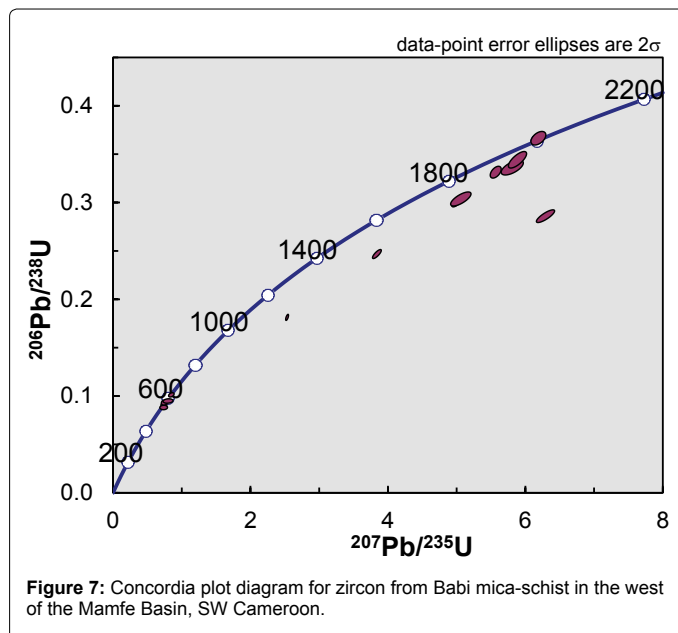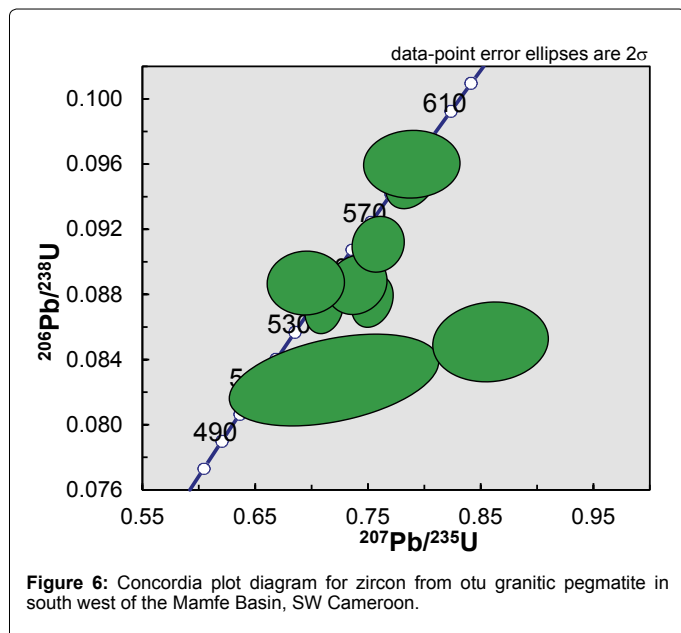**Zircon from Babi mica-schist:** The U, Th, and Pb contents range

Figure 5: CL images showing the internal texture of zircon from Babi mica-schistin the west of the Mamfe Basin, SW Cameroon.

Crystal and spot number	Analysis no.	$^{206}Pb/^{238}U$ Age (Ma) ± Prop_2SE	$^{207}Pb/^{235}U$ Age (Ma) ± Prop_2SE	$^{206}Pb/^{238}U$ Ratio ± Prop_2SE	$^{207}Pb/^{235}U$ Ratio ± Prop_2SE	$^{207}Pb/^{206}Pb$ Ratio ± Prop_2SE	$^{208}Pb/^{232}Th$ Ratio ± Prop_2SE	U (ppm)	Th (ppm)	Pb (ppm)	Th/U
Ot1-c	Output_1_1	537 ± 8.6	546.8 ± 7.2	0.08687 ± 0.0014	0.715 ± 0.012	0.06097 ± 0.00076	0.02785 ± 0.0008	168.2	155	40.8	0.921522
Ot1-r	Output_1_2	537.7 ± 8.1	534.8 ± 6.6	0.087 ± 0.0014	0.693 ± 0.011	0.05888 ± 0.00065	0.02607 ± 0.00087	148.8	99.4	26.1	0.668011
Ot2-r	Output_1_3	506.5 ± 11	490 ± 13	0.08175 ± 0.0018	0.622 ± 0.022	0.0558 ± 0.0013	0.0247 ± 0.0089	143	239.3	63.2	1.673427
Ot2-c	Output_1_4	584.4 ± 9.2	580.2 ± 7	0.0949 ± 0.0016	0.772 ± 0.013	0.05923 ± 0.00093	0.0294 ± 0.001	141.9	97	28.5	0.68358
Ot3-r	Output_1_5	589.1 ± 11	574 ± 11	0.0957 ± 0.0019	0.759 ± 0.019	0.0573 ± 0.0013	0.028 ± 0.0012	33.38	46.5	13.01	1.39305
Ot3-c	Output_1_6	639 ± 25	653 ± 29	0.1045 ± 0.0042	0.947 ± 0.066	0.0645 ± 0.0021	0.0334 ± 0.0038	16	18.3	6.86	1.14375
Ot4-r1	Output_1_7	545.5 ± 9.6	526.9 ± 9.1	0.0883 ± 0.0016	0.682 ± 0.016	0.0564 ± 0.0012	0.02662 ± 0.00094	56.9	90.2	22.1	1.585237
Ot4-r2	Output_1_8	545.4 ± 9.6	533 ± 9.5	0.0881 ± 0.0016	0.69 ± 0.016	0.0559 ± 0.0011	0.0268 ± 0.0011	47.4	55	14.1	1.160338
Ot5-r	Output_1_10	512 ± 12	493 ± 14	0.0828 ± 0.0021	0.631 ± 0.022	0.0558 ± 0.0013	0.0263 ± 0.0013	40.9	56.1	15.4	1.371638
Ot5-c	Output_1_9	550 ± 11	548 ± 14	0.0892 ± 0.0019	0.72 ± 0.023	0.0587 ± 0.0015	0.0297 ± 0.0028	51.8	62.2	41.4	1.200772
Ot6-r	Output_1_11	562 ± 9.4	557.9 ± 8.8	0.09101 ± 0.0016	0.729 ± 0.015	0.05869 ± 0.0079	0.02833 ± 0.00099	83	80.1	22.14	0.96506

Ot: zircon crystal from Otu; c: core; r: rim; Prop_2SE: propagated 2 standard error

Table 1: Quantified trace element abundance and U-Pb age for zircon crystals from Otu granitic pegmatite, SW of the Mamfe Basin.

Figure 6: Concordia plot diagram for zircon from otu granitic pegmatite in south west of the Mamfe Basin, SW Cameroon.

Figure 7: Concordia plot diagram for zircon from Babi mica-schist in the west of the Mamfe Basin, SW Cameroon.

Crystal and spot number	Analysis no.	$^{206}Pb/^{238}U$ Age (Ma) ± Prop_2SE	$^{207}Pb/^{235}U$ Age (Ma) ±Prop_2SE	$^{206}Pb/^{238}U$ Ratio ± Prop_2SE	$^{207}Pb/^{235}U$ Ratio ± Prop_2SE	$^{207}Pb/^{206}Pb$ Ratio ± Prop_2SE	$^{208}Pb/^{232}Th$ Ratio ± Prop_2SE	U (ppm)	Th (ppm)	Pb (ppm)	Th/U
Bab-3	Output_1_79	1857 ± 33	1919 ± 29	0.3334 ± 0.007	5.6 ± 0.2	0.1237 ± 0.0026	0.0957 ± 0.0029	50.7	86.3	82	1.70217
Bab-2c1	Output_1_77	1845 ± 24	1910 ± 10	0.3314 ± 0.0051	5.566 ± 0.068	0.12099 ± 0.0009	0.0937 ± 0.0027	158	72.5	64.3	0.458861
Bab-2r1	Output_1_78	1700 ± 24	1810.8 ± 12	0.3016 ± 0.0048	4.951 ± 0.07	0.11966 ± 0.0007	0.08684 ± 0.0026	270.8	41.92	38	0.154801
Bab-1c	Output_1_74	562 ± 12	544 ± 13	0.0909 ± 0.0019	0.706 ± 0.022	0.0562 ± 0.0012	0.0282 ± 0.0012	25.3	29.1	8.33	1.150198
Bab-1r1	Output_1_75	574 ± 12	559 ± 13	0.0931 ± 0.0021	0.736 ± 0.023	0.0564 ± 0.0012	0.0278 ± 0.0012	46.1	48.4	12.8	1.049892
Bab-1r2	Output_1_76	543 ± 12	526 ± 12	0.088 ± 0.002	0.676 ± 0.021	0.0558 ± 0.0012	0.0269 ± 0.0014	23.3	33.3	8.95	1.429185
Bab1-8	Output_1_87	1688 ± 32	1744 ± 27	0.299 ± 0.0064	4.57 ± 0.16	0.1115 ± 0.0025	0.0878 ± 0.0016	49	52.3	48.3	1.067347
Bab1-7c	Output_1_85	583.8 ± 9.8	577 ± 9.9	0.0948 ± 0.0017	0.77 ± 0.017	0.05926 ± 0.0009	0.0239 ± 0.0093	121	4.35	1.62	0.03595
Bab1-7r	Output_1_86	620.4 ± 10	615.5 ± 9.8	0.101 ± 0.0018	0.835 ± 0.018	0.06033 ± 0.0008.8	0.0467 ± 0.0074	89.1	14.6	4.77	0.163861
Bab1-6	Output_1_84	1536 ± 32	1668 ± 40	0.2963 ± 0.0062	4.23 ± 0.19	0.114 ± 0.0044	0.0443 ± 0.009	278.6	160.5	153.7	0.576095
Bab1-5r	Output_1_81	1043.9 ± 15	1050 ± 7.1	0.1758 ± 0.0028	1.815 ± 0.022	0.07514 ± 0.00026	0.754 ± 0.022	678	10.33	6.69	0.015236
Bab1-5c	Output_1_83	1418 ± 20	1598 ± 13	0.2462 ± 0.004	3.828 ± 0.058	0.11127 ± 0.00095	0.0745 ± 0.00082	593	11.66	10.23	0.019663
Bab1-4c	Output_1_80	2019 ± 30	2008 ± 18	0.3672 ± 0.0064	6.22 ± 0.12	0.123 ± 0.0014	0.1065 ± 0.0029	44	54.6	55.3	1.240909
Bab1-4r	Output_1_82	1919 ± 36	1954 ± 20	0.3451 ± 0.0075	5.86 ± 0.13	0.1232 ± 0.0012	0.0983 ± 0.0034	62.1	49.53	47.6	0.797585

Bab: zircon from Babi mica-schist; c: core; r: rim; Prop_2SE: propagated 2 standard error

Table 2: Quantified trace element abundance and U-Pb age for zircon crystals from Babi mica- schist in the west of the Mamfe Basin.

from 23 to 687 ppm, 4.0 to 161 ppm, and 1.0 to 154 ppm, respectively (Table 2). There is a slight variation of U, Th, and Pb content in each zircon crystal. The Th/U ratio ranges from 0.01 to 1.8 with some values being within range in metamorphic (< 0.07) [51] and magmatic zircon (≥ 0.5) [52] and 0.2-1.0 [11].

The U-Pb isotopic data in Table 2 are different with $^{206}Pb/^{238}U$ (0.09-0.4), $^{207}Pb/^{235}U$ (0.7 to 6.3), $^{207}Pb/^{206}Pb$ (0.05 to 0.16), and $^{208}Pb/^{232}Th$ (0.05 to 0. 12). The $^{206}Pb/^{238}U$ ages (543 ± 12- 2019 ± 30) and $^{207}Pb/^{235}U$ ages (526 ± 12 to 2008±18 Ma) are highly heterogeneous, they show some variation in age for the same zircon. They mainly date Paleoproterozoic (Statherian-Orosirian), Mesoproterozoic (Stenian-Calymmian), and Neoproterozoic (Edicarian) events. The plotted data in Figure 7 distinguish two main ages: (1) plotted on the discordia line and (2) plotted out of the discordia line. The group 1 plots, although slightly scattered, show some grouping with youngest and oldest ages well distinguished.

Discussions

Information on zircon texture, trace element geochemistry, and geochronology lead to their characterization and understand the history of their genesis.

Zircon from granitic pegmatite

In Otu pegmatite, zircons form euhedral elongated prismatic to pyramidal crystals with well-developed faces and some truncated edges (Figure 4). The presence of internal zoning in most of the crystals, typifies zircons from magmatic origin [2,3]. The grain size is above 100 μm, and are within the range of igneous zircon, mostly ranging from 20 to 250 μm [3]. The igneous nature of the zircons is clearly proven by the Th/U (0.6 to 1.7) which is above the mean ratio (≥0.5) of Konzett [52] magmatic zircon. Uranium (16 to 170 ppm) and Th (18 to 240 ppm) contents indicate their crustal origin as mantle zircons typically show very low U (<30 ppm) and Th (< 10 ppm) abundances

[4,16,32,35,36,53]. The relative low U (16 ppm) and Th (18.3 ppm) in Ot3-r cannot relate the crystallization of this crystal to mantle, as these elements content in Ot3-c of this same crystal, although relatively low, is more than values found mantle source zircon. This part of the zircon crystal probably form when the host solution was U-Th-depleted. The relative and general deplete in Th, U, and Pb abundance from core to rim of most grains can be due to the availability of these elements in each zircon growing solution and the degree of these elements substitution into zircon structure. Some of the crystals were grown in an environment more enriched in Th, U, and Pb than others. The degree of Th, U, and Pb substitution was much higher at the beginning of each crystal's crystallization than at the end. The U abundance in Ot1 exceeds 160 ppm, and lies within the range of many granitic zircons (154–4116 ppm). Those of other crystals and spots are below 145 ppm falling out of the range of the granitic zircon. Interpretation for this variation is difficult even though for Belousova [1], Th and U contents in igneous rocks are highly heterogeneous.

The variability of obtained ages for some zircons from Otu granitic pegmatite characterizes different period of crystallization (from Edicaran to Jiangshanian), and shows that the crystallization was progressive and took place in different period. This variation in age is not measured in all the zircon crystals. Two groups are distinguished: (1) zircon, with one stage crystallization and (2) zircon, with two stages (progressive) crystallization. The group 1 zircon crystals with no age variation were not mainly crystallized in a progressive manner. If base on the $^{206}Pb/^{238}U$ ages (Table 1) the crystallization of some of the group 2 zircons probably started in Later Edicaran (or Cryogenian) and ended in Middle Cambrian, or ended in Early Cambrian if $^{207}Pb/^{235}U$ ages are considered. The obtained ages for the studied zircon crystals are close to most age published for Precambrian age rocks: (e.g., 520± 20 Ma for Poli and 498 ± 5 Ma for Lom: [43] and 569 ± 12 to 558 ± 24 Ma, and 533 ± 12 to 524 ± 28 Ma for Nkambe: [44,45]) within the Central African Fold Belt. This similarity in age suggests that the Otu granitic pegmatite and part of the Precambrian age rocks found within the Cameroon Mobile Belt were grown at the same period. The age of part of the oldest zircon crystals (e.g., 574 ± 11 Ma) is close to oldest (569 ± 12 Ma) for Tetsopgang [45] foliated biotite monzogranite outcropping in Nkambe, suggested to having crystallized during a collisional event. The Otu pegmatite zircons may date a continental granitic rocks crystallized during the Panafrican (Ediacaran) collisional event. If collusion is considered, it is possible that this collusion started in Cryogenian and ended in Early Cambrian. This interpretation is based on age variation, but not zircon textural future, or micropetro-structural analysis of rock fragments.

Zircon from Babi mica-schist

Zircons form sub-hedral to euhedral crystals, or crystal fragments while, others form rounded grains with soccer-ball or ovoid shape (Figure 5). The rounded soccer-ball shape of some of the zircons may typify metamorphic feature, if based on Pupin [3] and Corfu [5] zircon internal morphological classification. The metamorphic nature is visible on crystal with over-growing and preserved core. These two distinctive morphologies characterize zircon crystallized in medium-grade metamorphic rocks and protolith re-crystallization. The sub-hedral and euhedral feature of some of the zircons, added to their weak internal zoning seem symptomatic of their magmatic origin [2]. The fragmented aspect of some zircons can be due to brittle syn-tectonic broken, or before metamorphism fracturing during long distance transportation in river (inherited zircon) [3,5,50]. The internal

structure of the Babi zircon is composed of inherited and authigenic new crystallized zircons.

The variable U (25 to 679 ppm) and Th (4 to 161 ppm) contents may characterize crystallization from different environments. The U and Th abundance are dominantly within the range limit in crustal derived zircons if based on results presented in the above paragraphs or on those presented by Heaman [16], Belousova [4], and Kanouo [35,36]. Some crystals with Th/U ratio (<0.04) are metamorphic crystallized zircon, as Th/U ratios for metamorphic melt crystallized zircon are below 0.07 [51]. The Th/U ratios (> 0.5) in part of those zircon crystals are above the mean ratio in of Konzett [52] igneous zircon, and above the mean value (0.4) in granitic zircons. They may represent igneous crystallized zircons. The igneous heritage is supported by the U contents within the range limit in magmatic zircon. The Babi mica-schist zircon crystals are composed of three populations: (1) inherited magmatic zircons, (2) syn-host-rock magmatic zircons, and (3) syn-host-rock metamorphic zircons [53].

The U-Pb ages range from 2019 ± 30 to 543 ± 12 Ma ($^{206}Pb/^{238}U$ ages) and 2008 ± 18 to 526 ± 12 Ma ($^{207}Pb/^{235}U$ ages). This heterogeneity in age shows that the Babi mica-schist zircons were not crystallized at the same period. Part of those zircons is inherited, while, others are not. The inherited nature of part of the zircon is confirmed by the measured age and geochemical features. Those with age ranging from 2019 to 1688 Ma ($^{206}Pb/^{238}U$) or 2008 to 1668 Ma ($^{207}Pb/^{235}U$) are the oldest zircons. Their geochemical features in Table 2 show that they are dominantly of igneous crustal crystallization. The magmatic nature of those zircons shows that they were not grown in the Babi mica-schist, as mica-schists are regional metamorphic rocks. They are pre-sedimentary and pre-metamorphic grains inherited from the source rock(s) of the transformed materials that formed the Babi mica-schist. The crystallization period of these zircons is Paleoproterozoic (Orosirian and/or Statherian). It is not easy to know if those zircons were sorted from the same rock or from different rocks. Due to the age gab, it is probable that the zircons were sorted from different rocks with some of those rocks being more U, Th and Pb enriched and older than others [54]. The age of Statherian zircon crystals is closed to the inherited magmatic age (1617 ± 16 Ma) presented by Tchakounté [49] for metasediments in the Bafia group. This similarity in age suggests that the source rock of the studied Statherian zircon and that of Bafia zircon crystallized at the same period. The age of the oldest Orosirian zircons is close to 2.1 Ga age for the garnet amphibolites and tonalitic to trondhjemitic gneisses of Tonga published by Njiosseu [48]. The same interpretation can be given to this age similarity [55].

The Calymmian (1418 ± 20 Ma: $^{206}Pb/^{238}U$ or 1598± 13 Ma: $^{207}Pb/^{235}U$) zircon and part of Edicaran (583.8 ± 9.8 Ma: $^{206}Pb/^{238}U$ or 577± 9.9 Ma: $^{207}Pb/^{235}U$) crystals with Th/U 0.07 are metamorphic, if based Rubatto [51] zircon classification. These zircons are syn-metamorphic zircons which crystallized in the Babi mica-schist. Their crystallization periods are different as they have different age. The first crystallization period took place during the Late Mesoproterozoic and the second during the Early Neoproterozoic. Two ages (Calymmian and Stenian) are recorded by the Late Mesoproterozoic zircon, suggesting that the crystallization started during the Calymmian and ended during Stenian. The Late Mesoproterozoic zircons may date formation period of Babi mica-schist, from metamorphic transformation of the accumulated Paleoproterozoic sediments. The sedimentation period of the transformed sediments is not easy to determine, but, may be pre-Calymmian. This Calymmian metamorphic period is different and younger than the Eburnean (2400-1800 Ma, Rb-Sr whole-rock dating)

[43]. Other metamorphic period recorded by Babi mica-schist is the Edicaran event. This Edicaran age is close to most Late Neoproterozoic (Panafrican) ages measured in rocks found within the Central African Fold Belt [56]. This age is also similar to that of most zircon in the Otu granitic pegmatite, showing that the Otu granitic pegmatite was formed at the same time as the second metamorphic phase that affected the Babi mica-schist. If based on the collisional interpretation given to most Edicaran age rocks within Cameroon Mobile Zone, it is probable, that the second metamorphic phase registered by the Babi mica-schist took place during this collision. The Babi mica-schist recorded two metamorphic events: (1) the Calymmian transformation of the Paleoproterozoic sediments and (2) Edicaran collisional and partially re-crystallization of the Calymmian metamorphic rock. The Edicaran magmatic zircon hosted in the Babi mica-schist may be anatectic crystal formed from a melt by partial fusion of the host rock during the Pan-African collisional orogeny [57].

Conclusions

The Otu granitic pegmatite is crustal derived rock formed during the Edicaran to Cambrian period probably from a collisional event. The Babi mica-schist is a rock form by metamorphic transformation of Paleoproterozoic detrital sediments sorted from magmatic sources. It recorded two metamorphic events: the Calymmian transformation of the Paleoproterozoic sediments and the Edicaran partial transformation of the Calymmian during Pan-African collisional orogeny. This rock also experience partial melting and magmatic zircon authigenic crystallization during Edicaran period.

Acknowledgements

References

1. Belousova AE, Griffin LW, O Reilly YS, Fisher IN (2002) Igneous zircon: Trace element composition as an indicator of source rock type. J Min and Petro 143: 602-622.

2. Hoskin PWO, Schaltegger U (2003) The composition of zircon and igneous and metamorphic petrogenesis. Rev in Min and Geochem 53: 27-55.

3. Pupin JP (1980) Zircon and granite petrology. Con Min and Petr 73: 207-220.

4. Belousova AE, Griffin LW, Pearson JN (1998) Trace element composition and cathodoluminesence properties of southern African kimberlitic zircons. Min Mag 62: 355-366.

5. Corfu F, Hanchar JM, Hoskin PWO, Kinny P (2003) Atlas of zircon texture In: Hanchar, J.H. and Hoskin, P. W. O edition. Zircon Reviews in Mineralogy and Geochemistry, 53, 469-500.

6. Yang K, Bodnar RJ (1994) Magmatic-hydrothermal evolution in the "Bottoms" of porphyry copper systems: evidence from silicate melt and aqueous fluid inclusions in granitoid intrusions in the Gyeongsang Basin, South Korea. Int Geo Rev 36: 608-628.

7. Devine JD, Gardener JE, Brack HP, Layne GD, Rutherford MJ, et al. (1995) Comparison of microanalytical methods for estimating H2O contents of silicic volcanic glasses. American Mineralogist 80: 319-328.

8. Scoates JS, Chamberlain KR (1995) Baddeleyite (ZrO2) and zircon (ZrSiO4) from anorthositic rocks of the Laramie anorthosite complex, Wyoming: petrologic consequences and U-Pb ages. American Mineralogy, 88: 1317-1327.

9. Gebauer D, Schertl HP, Brix M, Schreyer W (1997) 35 Ma old ultrahigh-pressure metamorphism and evidence for very rapid exhumation in the Dora Maira Massif, Western Alps. Lithos, 41: 5-24.

10. Thomas BJ, Bodnar JR, Shimizu N, Chesner CA (2002) Melt inclusions in zircon. Reviews in Mineralogy and Geochemistry 53: 63-83.

11. Kirkland CL, Smithies RH, Taylor RJM, Evans N, McDonald B, et al. (2015) Zircon Th/U ratios in magmatic environs. Lithos 212: 397–414.

12. Dickin PA (1995) Radiogenic isotope geology. [2 Edition] Cambridge University Press, pp.489.

13. Wan-Chang H, Turek A, Bin Kim C (2003) U-Pb zircon geochronology and Sm-Nd-Pb- isotopic constraint for Precambrian plutonic rocks in the northeastern part of Ryeongnam massif, Korea. Geochem J 37: 471-491.

14. Yuan H, Gao S, Liu X, Li H, Gunther D, et al. (2004) Accurate U-Pb age and trace element determination of zircon by Lased Ablation-Inductively Couple Masse Spectrometry. Geostadars and Geoanalytical Res 28: 358-370.

15. McInnes AIB, Evans JN, McDonald JB, Kinny DP, Jakimowicz J, et al. (2009) Zircon U-Th-Pb-He double dating of Merlin kimberlite field, Northern Territory, Australia. Lithos 1125: 592-599.

16. Heaman LM, Bowins R, Crocket J (1990) The chemical composition of igneous zircon suites: Implications for geochemical tracer studies. Geochimica et Cosmochimica Acta, 54, 1597-1607.

17. Xia X, Sun M, Zhao G, Luo Y (2006) LA-ICP-MS U-Pb geochronology of detrital zircons from the Jining Complex, North China Craton and its tectonic significance. Chinese Science Bulletin 59: 1425-1437.

18. Wilson D (1928) Notes on the geology of the Mamfe Division, Cameroon SW province. Occasional papers. Geologic Survey of Nigeria no 6.

19. Le Fur Y (1965) Special report on corundum gems research. Cretaceous-Base Mission, Mamfé YAO 666A8. Archives BRGM. DMG / MINEE.

20. Dumort JC (1968) Geological map of recognition of Cameroon at scale 1/500000 sheet Douala-West, with explanatory note. National printing house, Yaoundé, Cameroon, pp.69.

21. Regnoult JM (1986) Geological Synthesis of Cameroon. Directorate of Mines and Geology, Yaoundé, Cameroon pp.119.

22. Njoh OA, Nforsi MB, Datcheu JN (2015) Aptian-Late Cenomanian Fluvio-Lacustrine Lithofacies and Palynomorphs from Mamfe Basin, Southwest Cameroon, West Africa. Int J Geo 6: 795-811.

23. Ajonina NH (2016) Evolution of Cretaceous sediments in the Mamfe Basin, SW Cameroon: Depositional environments, Palynostratigraphy, and Paleogeography. Unpubl. PhD Thesis. Univ of Hamburg. pp.202.

24. Kanouo SN (2014) Geology of the Western Mamfe corundum deposits, SW region Cameroon: Petrography, geochemistry, geochronology, genesis, and origin. unpubl. PhD Thesis. Univ de Yaounde I pp.225.

25. Eyong TJ (2003) Lithostratigraphy of the Mamfe Cretaceous Basin. South West Province of Cameroon-West Africa. Ph.D. Thesis, University of Leeds, Great Britain, pp.256.

26. Eseme E, Littke R, Agyingi MC (2006) Geochemical characterization of Cretaceous black shale from the Mamfe Basin, Cameroon. Petroleum Geosciences 12: 69-74.

27. Njoh OA, Njie SM (2016) Hydrocarbon source rock potential of the lacustrine black shale unit, Mamfe Basin, Cameroon, West Africa. Earth Sci Res 6: 217-230.

28. Martin EJ, Menken FE, Djomeni A, Fowe PG, Ntamak-Nida JM (2017) Dinosaur trackways from the early Late Cretaceous of 1 western Cameroon. J Afr Earth Sci 134: 213-221.

29. Eseme E, Agyingi MC, Foba-Tendo J (2002) Geochemistry and genesis of brine emanations from cretaceous strata of the Mamfe basin, Cameroon. J African Earth Sci 35: 467-476.

30. Eyong TJ, Wignall P, Fantong YW, Best J, Hell VJ, et al. (2013) Paragenetic sequences of carbonate and sulphide minerals of the Mamfe Basin (Cameroon): Indicators of palaeo-fluids, palaeo-oxygene levels and diagenetic zones. J African Earth Sci 86: 25-44.

31. Laplaine L, Soba D (1967) Geological Survey Report for Years 1965-1966-1967, prospecting of sapphires in the Cretaceous basin of Mamfé. Archives BRGM /DMG/ MINMEE.

32. Kanouo SN, Zaw K, Yongue FR, Sutherland LF, Meffre S, et al. (2012a) U-Pb zircon age constraining the source and provenance of gem-bearing late Cenozoic detrital deposit, Mamfe Basin, SW Cameroon. Resour. Geol 62: 316-324.

33. Kanouo SN, Yongue FR, Shouyu C, Njonfang E, Ma C, et al. (2012b) Greyish

black rutile megaclasts from the Nsanaragati Gem Placer, SWCameroon: Geochemical features and genesis. J Geogr Geol 3: 134-146.

34. Kanouo SN, Zaw K, Yongue FR, Sutherland LF, Meffre S, et al. (2012c) Detrital mineral morphology and geochemistry: Methods to characterize and constrain the origin of the Nsanaragati blue sapphires, south-western region of Cameroon. J Afr Earth Sci 70: 18-23.

35. Kanouo SN, Yongue FR, Ekomane E, Njonfang E, Ma C (2015) U-Pb ages for zircon grains from Nsanaragati Alluvial Gem Placers: Its correlation to the source rocks. Resour Geol 65: 103-121.

36. Kanouo SN, Ekomane E, Yongue FR, Njonfang E, Zaw K, et al. (2016) Trace elements in corundum, chrysoberyl, and zircon: Application to mineral exploration and provenance study of the western Mamfe gem clastic deposits (SW Cameroon, Central Africa). J African Earth Sci 113: 35-50.

37. Njonfang E, Moreau C (1996) The Mineralogy and geochemistry of a subvolcanic alkaline complex from the Cameroon line, the Nda Ali massif, South-West Cameroon. J African Earth Sci 22: 113-132.

38. Kanouo SN, Yongue FR, Ghogomu RT, Njonfang E, Yomeun BS, et al. (2017) Petro-geochemistry, Genesis and Economic Aspects of Mafic Volcanic Rocks in the West and Southern Part of The Mamfe Basin (SW Cameroon, Central Africa). J Geol Geophys.

39. Toteu FS, Penaye J, Poudjom-Djomani Y (2004) Geodynamic evolution of the Pan-African belt in central Africa with special reference to Cameroon. J African Earth Sci 41: 73-85.

40. Abbelsalam GM, Liégeois PJ, Stern JR (2002) The Saharan Metacraton. J African Earth Sci 34: 119-136.

41. Ngako V, NjonfangE, Affaton P (2008) Pan-African tectonics in North-Western Cameroon: Implication for the history of the Western Gondwana. Gondwana Research 14: 509-522.

42. Toteu FS, Van Schmus WR, Penaye J, Michard A (2001) New U-Pb and Sm-Nd data from north-central Cameroon and it bearing on the Pre-Pan African history of Central African. Precambrian Research 108: 45-73.

43. Lasserre M, Soba D (1976) Ages Cambrien Nyibi and Kongolo granites (Centre-Est Cameroun). Accounts Acad Sci 283: 1695-1698.

44. Tetsopgang S, Suzuki K, Adachi M (1999) Preliminary CHIME dating of granites from Nkambe area, northwestern Cameroon. J Earth and Plan Sci 46: 57-70.

45. Tetsopgang S, Suzuki K, Njonfang E (2008) Petrology and CHIME geochronology of Pan-African high K and Sr/Y granitoids in the Nkambe area, Cameroon. Gondwana Research 14: 686-699.

46. Tagne-Kamga G (2003) Petrogenesis of the Neoproterozoic Ngondo igneous plutonic complex (Cameroon, west central Africa): A case of late collisional ferro-potassic magmatism. J African Earth Sci 36: 149-171.

47. Nzenti JP, Barbey P, Macaudiere J, Soba D (1988) Origin and evolution of the Late Precambrian high-grade Yaoundé gneisses (Cameroon). Precambrian Research 38: 91-109.

48. Njiosseu TLE, Nzenti PJ, NjankoT, Kapajika B, Nédélec A, et al. (2005) New U-Pb zircon ages from Tonga (Cameroon): Coexisting Eburnian-Transmazonian (2.1 Ga) and Pan-African (0.6 Ga) imprints. Comptes Rendus Geosci 337: 551-562.

49. Tchakounté NJ, Toteu FS, Van Schmus RW, Penaye J, Deloule E, et al. (2007) Evidence of ca 1.6 Ga detrital zircon in Bafia group (Cameroon): Implication for chronostratigraphy of the Pan-African Belt north of the Congo craton. Com Ren Geo 339: 132-142.

50. Robert MF, Finger F (1997) Do U-Pb zircon ages from granulites reflect peak metamorphic conditions? J Geo 25: 319-322.

51. Mcfarlane MRC, Yan L (2012) U-Pb Geochronology using 193 nm Excimer LA-ICP-MS optimized for in situ accessory mineral dating in thin sections. Geoscience Canada 39; 158-172.

52. Rubatto D (2002) Zircon trace element geochemistry: Portioning with garnet and the link between U-Pb age and metamorphism. J Chem Geo 184:123-138.

53. Konzett J, Armstrong RA, Sweeny RJ, Compston W (1998) The timing of Marid suite metasomatism in the Kaapvaal mantle: an ion probe study of zircons from Marid xenoliths. Earth and Planetary Sci Let 160: 133-145.

54. Mbih PK, Meffre S, Rose Fouateu Yongue FR, Kanouo SN, Thomson J, et al. (2016) Chemistry and origin of the Mayo Kila sapphires, NW region Cameroon (Central Africa): Their possible relationship with the Cameroon volcanic line. J African Earth Sci 118: 263-273.

55. Belousova EA (2000) Trace elements in zircon and apatite: Application to petrogenesis and mineral exploration. PhD Thesis, Macquarie University, Australia pp.310.

56. Belousova EA, Griffin WL, Suzanne YO (2005) Zircon crystal morphology, trace element signatures and Hf isotopic composition as tool for petrogenetic modeling: Examples. J Petrology 47: 329-353.

57. Kanouo SN (2008) Geological study of the sapphire mineralization indexes in the southern part of the Mamfe sedimentary basin. University of Yaoundé I, Memoire of D.E.A pp.91.